Journal of Applied Electrochemistry (2006) 36:807–812
DOI 10.1007/s10800-006-9137-8

Electrodeposition of Pd–Ag alloy nanowires on highly oriented pyrolytic graphite

YAOKUN XIAO[1], BAICHENG WENG[1], GANG YU[1,*], JINYIN WANG[2], BONIAN HU[2] and ZONGZHANG CHEN[1]
[1]*State Key Laboratory of Chemo/Biosensing and Chemometrics, College of Chemistry and Chemical Engineering, Hunan University, Changsha 410082, China*
[2]*Hunan College of Building Materials, Hengyang 421008, China*
*(*author for correspondence, tel.: +86-0731-8821770, fax: +86-0731-8713642, e-mail: yuganghnu@163.com)*

Received 18 May 2005; accepted in revised form 1 March 2006

Key words: alloy nanowires, electrodeposition, highly oriented pyrolytic graphite, Pd–Ag

Abstract

This paper reports findings of an investigation of Pd–Ag alloy nanowires on the step edges of highly oriented pyrolytic graphite (HOPG) by electrochemical deposition at room temperature. Scanning electron microscopy (SEM) images reveal that these alloy nanowires (109–430 nm) are uniform in diameter, and have lengths up to 100–500 μm. The electrodeposition process involves the initial formation of nanowires induced at the step edges of the oxidized HOPG substrate at a very negative potential and subsequent growth at a constant low current density to coalesce the discontinuous nanowires. Alloy nanowires with a 20–25% silver content can be obtained when the ratio of Pd and Ag in the solution is carefully controlled. The SEM images demonstrate that the alloy nanowire arrays are continuous, parallel, ordered, well-aligned and have a narrow distribution of diameters. The Pd–Ag alloy nanowire arrays are promising materials for fabricating hydrogen nanosensors.

1. Introduction

Hydrogen is emerging as a primary fuel source to replace oil-based fuels. Since this gas is not sensed by the human olfactory system and it has a wide range of concentration for ignition in air (4–75%) [1], the need for leak detection technology is especially important in places where large volumes of hydrogen are handled. For rapid response in a complex environment, palladium metal and alloys are used as sensing materials. The advantage of the palladium-based technology is its independence from the local environment, as well as its small size and ability to be used at high pressures. The surface of palladium acts catalytically to break the H–H bond in diatomic hydrogen and allows the atomic hydrogen to diffuse into the material. Palladium can dissolve hydrogen of more than 600 times its volume. The electrical resistivity of the metal changes proportionally with the level of dissolved hydrogen, which makes it highly desirable as a hydrogen sensing material.

The development of nanometer-scale materials offers new opportunities for the construction of sensors and electronic devices. Nanowires have attracted particular attention, because of their unusual properties and potential utilization in electric, magnetic, optical, and micromechanical devices [2–7]. The sensors based on Pd mesowire arrays fabricated by Penner and co-workers were shown to respond to hydrogen reversibly. The sensors are highly sensitive and selective [3, 4]. However, one problem is blistering of Pd films at high concentrations of hydrogen [1]. To solve this problem, one effective method is adding silver into the metal to prevent it from the transition of Pd–H compound from α phase to β phase. There are therefore advantages to fabricate Pd–Ag alloy nanowires in comparison with pure Pd nanowires for the application in hydrogen sensors. Considerable efforts have been made on the synthesis of nanowires with different compositions using physical evaporation [8], template (AAO or AAM template and surface template) [5, 6, 9–16] and other methods [17, 18]. The successful synthesis of Pd–Ag alloy nanowires has not been reported up till now. This paper reports the results of our successful fabrication of Pd–Ag alloy nanowires on the step edge of highly oriented pyrolytic graphite (HOPG) by electrochemical deposition at room temperature. In order to fabricate linear and well-aligned nanowires of Pd–Ag alloy, the step edges of HOPG are used as the template for the electrodeposition of Pd–Ag alloy nanowires. The deposition processes and the dependence of alloy composition on the concentration ratio of Pd and Ag in the solution have been examined for the fabrication of Pd–Ag alloy nanowires.

2. Experimental

2.1. *Materials*

$Pd(NO_3)_2$ (AR) was obtained from Kunming Institute of noble metals, Yunnan, China. The $AgNO_3$ (AR) and NH_4NO_3 (AR) were obtained in the reagent factory of Shanghai, China. They were dissolved in double distilled water. The working electrode was a piece of HOPG (ZYA μ-masch MikroMasch) substrate ($10 \times 3 \times 1$ mm^3 with an effective area of 0.1 cm^2).

2.2. *Electrodeposition method*

The plating solutions were purged with pure Ar (99.999%) for 15 minutes before experiments. Nanowires were electrodeposited on the basal plane of ZYA grade HOPG which was cleaved with a ''Newgen'' brand adhesive tape prior to use. All deposition experiments were carried out in three electrode cells with a Pt foil as counter electrode and a saturated calomel electrode (SCE) as reference electrode. After deposition, the HOPG working electrode with alloy nanowires deposited was moved from the plating solution, carefully rinsed with double distilled water and dried in air prior to characterization.

Potential or current pulses were applied using a CHI660B electrochemical workstation (CH Instruments Shanghai China). The alloy nanowires were analyzed by scanning electron microscopy (SEM) using JEOL JSM-5600LV microscope equipped with energy dispersed X-ray spectrometer (EDX) (Noran Vantage 4105).

3. Results and discussion

Various plating solutions were tested, which are summarized in Table 1. Effects of the concentration of NH_4NO_3 and the Pd/Ag concentration ratio on the morphologies and composition of alloy nanowires were investigated. The results are discussed in the following sub-sections.

3.1. *Effect of NH_4NO_3 electrolyte in plating solution*

It is known that the alloy of Pd and Ag can be obtained by adding $NH_3 \cdot H_2O$ in pH ranges of 2–3 or 8–11 [19, 20]. In a mixture of $Pd(NO_3)_2$ and $AgNO_3$ without NH_4^+ or NH_3, the formation of dense particles on the terrace of HOPG was usually found (Figure 1A). It is difficult to electro-deposit nanowires in the basic mixture of $Pd(NO_3)_2$ and $AgNO_3$ obtained by adding $NH_3 \cdot H_2O$. Pd–Ag alloy grew into dendrites and sheet crystals, as shown in Figure 1B.

If the plating solution is composed of $Pd(NO_3)_2$, $AgNO_3$ and NH_4NO_3, NH_4^+ can be further ionized according to the following reaction:

$$NH_4^+ \rightleftharpoons NH_3 + H^+ \quad (K = 9.24) \tag{1}$$

The reaction product NH_3 will complex with Pd^{2+} and Ag^+ based on the following reactions:

$$mNH_3 + Pd^{2+} \rightleftharpoons Pd(NH_3)_m^{2+} \quad \beta_m \tag{1}$$

$$nNH_3 + Ag^+ \rightleftharpoons Ag(NH_3)_n^+ \quad \beta_n^* \tag{1}$$

In the above equations, $m = 1, 2, 3, 4$; $n = 1, 2$; $\lg \beta_1 = 9.6 > \lg K$, $\lg \beta_1^* = 3.24 > \lg K$. When NH_4NO_3 is added into the Pd–Ag plating solution, some of the Pd^{2+} and Ag^+ ions are complexed with ionized NH_3. NH_4NO_3 can increase the solution conductance and reduce the deposition rate of Pd^{2+} and Ag^+. The SEM images in Figure 2A, B and C show various morphologies of

Table 1. A summary of various plating solutions with different Pd/Ag concentration ratio and NH_4NO_3 concentration

No.	Solutions of various Pd/Ag ion concentration ratio		Solutions of various NH_4NO_3 concentration	
1	50:1	$AgNO_3$ Variable	0.5 M	NH_4NO_3 Variable
2	25:1	$Pd(NO_3)_2$ 0.5 mM	1.0 M	$AgNO_3$ 0.033 mM
3	15:1	NH_4NO_3 2.0 M	1.5 M	$Pd(NO_3)_2$ 0.5 mM
4	10:1	pH = 2–3	2.0 M	Ratio of Pd/Ag ion 15:1
5	1:1		2.5 M	pH = 2–3

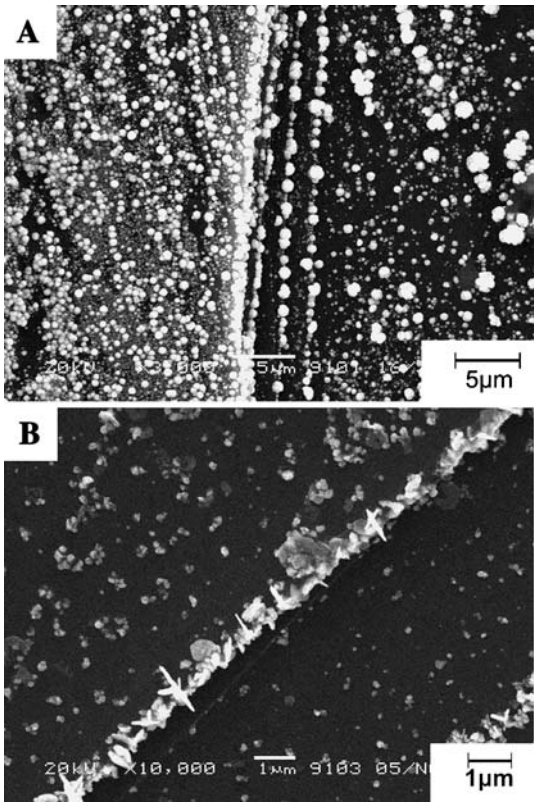

Fig. 1. Morphologies of Pd–Ag alloy electrodeposited in the mixtures of $Pd(NO_3)_2$ and $AgNO_3$ without $NH_3 \cdot H_2O$ (A) or with $NH_3 \cdot H_2O$ (B) (A: $E_{ox} = 0.8$ V$_{SCE}$, $t_{ox} = 10$ s, $E_{nucl} = 0.26$ V$_{SCE}$, $t_{nucl} = 5$ ms, $i_{growth} = -20$ μA cm^{-2} for 600 s; B: $E_{ox} = 0.8$ V$_{SCE}$, $t_{ox} = 10$ s, $E_{nucl} = -0.8$ V$_{SCE}$, $t_{nucl} = 5$ ms, $i_{growth} = -100$ μA cm^{-2} for 1800 s).

nanowires obtained in different concentrations of NH_4NO_3 under the same electrodeposition condition.

Using the data in Figure 2, the dependence of nucleation density on terraces and the diameters of the initially formed particles on the NH_4NO_3 concentration in the plating solution are plotted (Figure 3). The nucleation density and the particle diameters obviously decrease with the increase in NH_4NO_3 concentration. Well-defined morphology of the nanowires can be obtained in the plating solution with the higher concentration of NH_4NO_3. It is important to note that the effect of NH_4NO_3 is not significant if its concentration is beyond 2 M. The Pd–Ag plating solution containing 2 M NH_4NO_3 was found to be preferable for electrodeposition of Pd–Ag alloy nanowires.

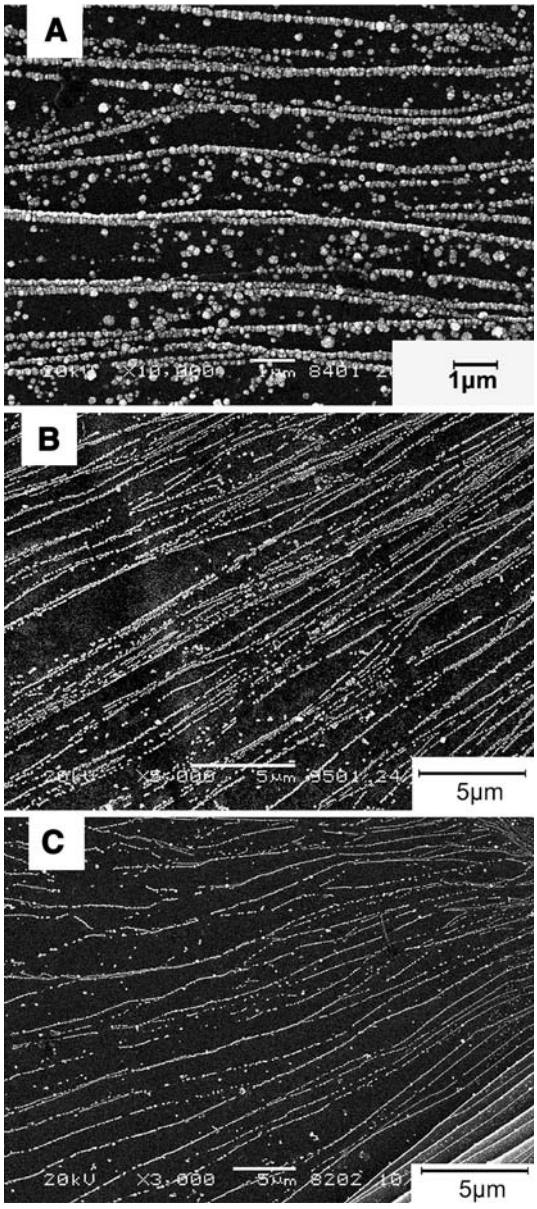

Fig. 2. SEM images of Pd–Ag nanowires obtained in the solutions containing NH_4NO_3 of 0.5 M (A), 1.5 M (B), 2.5 M (C) ($E_{ox} = 0.8$ V, $t_{ox} = 25$ s; $E_{nucl.} = -1.0$ V, $t_{nucl.} = 0.6$ s; $i_{growth} = -20$ μA cm^{-2}, $t_{growth} = 600$ s, c [$Pd(NO_3)_2$] = 0.5 mM, c ($AgNO_3$) = 0.033 mM, pH = 2–3).

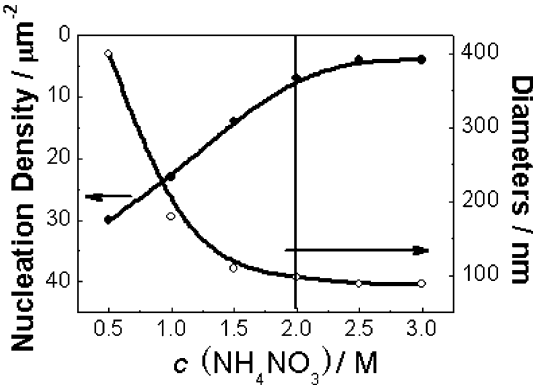

Fig. 3. Dependence of the nucleation density on terraces and the diameters of the nucleation particles on the concentration of NH_4NO_3 in the plating solution.

3.2. *Effect of the Pd/Ag concentration ratio*

The Pd and Ag composition in the alloy can be altered by adjusting the Pd/Ag concentration ratio in the plating solution. Figure 4 shows the dependence of silver content in the nanowires on the Pd/Ag concentration ratio in the solution (at 0.5 mM $Pd(NO_3)_2$). The content of Ag in the alloy decreases dramatically with the increase in the Pd/Ag concentration ratio in the solution. It reaches 23% Ag content at the Pd/Ag ratio of 15:1.

3.3. *Effect of the electrodeposition parameters*

The oxidation process is known to be responsible for the growth of nanowires at the step edges of HOPG [21–24]. The HOPG may be slowly oxidized at the potential of 0.8–1.1 V, as shown in Figure 5. The potential is too low to oxidize carbon on terraces in any significant way. However, carbon at the steps is easily oxidized to produce oxygen-containing functionalities preferentially at steps. The current pulse at 1.1 V shown in Figure 5 was caused by graphite decomposition. The steps thus oxidized can increase the affinity of metal adatoms,

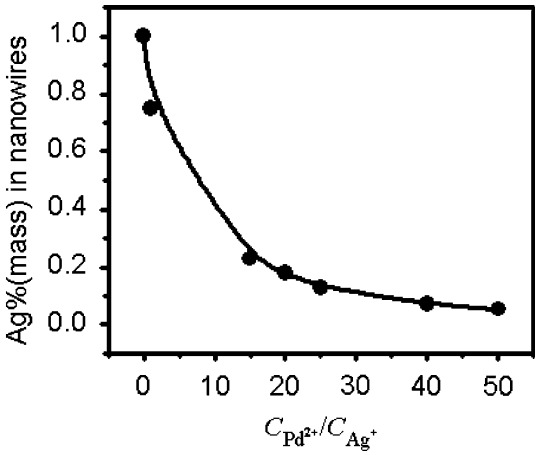

Fig. 4. Dependence of Ag content in alloy nanowires on the concentration ratio of Pd/Ag in the plating solution.

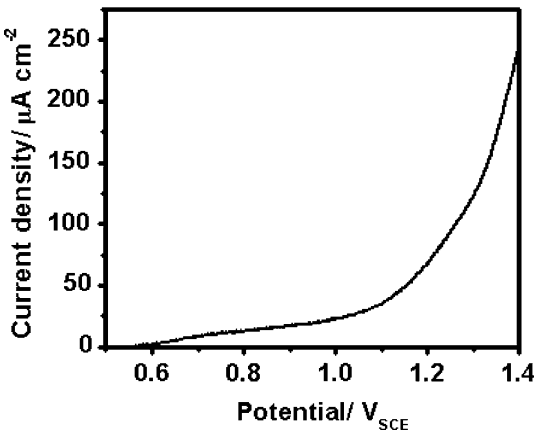

Fig. 5. Curve of anodic polarization for HOPG in the plating solution composed of 0.5 mM $Pd(NO_3)_2$, 0.033 mM $AgNO_3$, and 2.0 M, NH_4NO_3 (pH = 2.6).

reduce the nucleation overpotential, and increase the nucleation density along step edges [12].

It is usually expected that nanowires are deposited at the step edges of HOPG. However, some particles were observed on the terrace of HOPG, shown in Figure 6A, B. The results demonstrate the formation of the step edges of HOPG after oxidizing at the potential of 0.8 V. These step edges favor the formation of the nanowires. Many spot and line defects were also observed on the terraces of HOPG, which implied the presence of other sites for metal nucleation. Therefore, not only nanowires have been observed on the steps, but also metal particles were detected on the terraces.

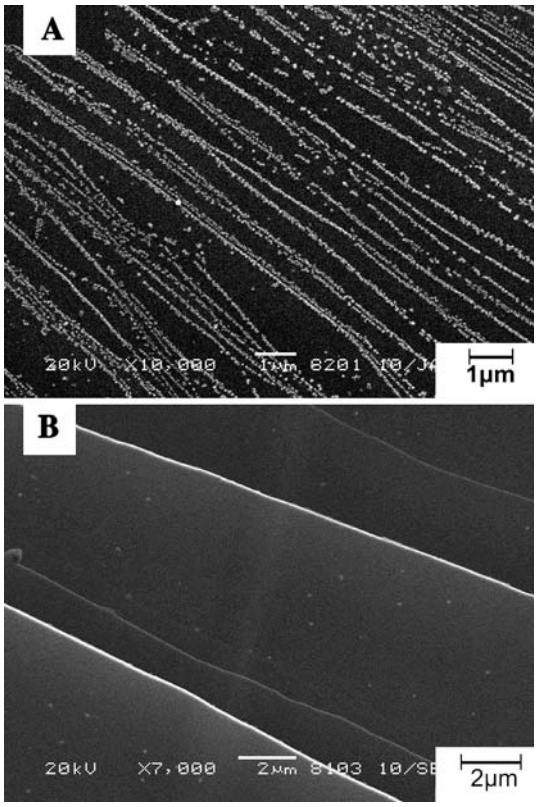

Fig. 6. SEM images for (A) Pd–Ag alloy nanowires on the HOPG, and (B) bare HOPG.

The nucleation step is important for the formation of a high density of metal nuclei along step edges which function as "skeletons" of nanowires. It is very important to keep a high linear density of metal nuclei along step edges ($>20\ \mu m^{-1}$) without producing rapid nucleation of metal on terraces in order to get good Pd–Ag alloy nanowires [21]. Values of E_{nucl}, which are more positive than −1.0 V, were found to produce a low linear density of metal nuclei along the step edges, Thus, the coalescence of nuclei particles into smooth nanowires can not be realized by growth at low current density for a long time.

Under a potential more negative than −1.0 V in the low metal concentration solution, the metal ions are rapidly depleted near the surface of the graphite electrode and the concentration polarization occurs. In Figure 7, the current density versus time transient is plotted at potential −1.0 V. The transient is found to be linear to $t^{-1/2}$, indicating the control by limited mixed diffusion [25]. The electrodeposition reaction rates of Pd and Ag are all very fast. The increase of the overpotential raised did not increase the electrodeposition rates of Pd and Ag. Therefore, the composition in the alloy is not changed. The application of a too large overpotential causes hydrogen evolution and excessive nucleation of metal particles on terraces. We found that the applied nucleation potential between −1.0 V and −1.5 V for 0.2–0.6 s is the optimum formation condition of nanowires. The hydrogen evolved on the surface under the nucleation potential does not influence the structure of the nanowires in such short nucleation time. As shown in Figure 8, the preferential nucleation and growth at step edges occur at −1.0 V for 0.6 s and the discontinuous nanowires with the diameter of less than 100 nm are formed.

Experiments also showed that the nucleated particles underwent coalescence into smooth nanowires when the deposition was carried out at constant low current density of $-20\ \mu A\ cm^{-2}$ for 2400 s, as shown in Figure 9. The spaces between the neighboring particles were not coalesced by growth for hours if a growth current density lower than $-20\ \mu A\ cm^{-2}$ was applied. Nevertheless,

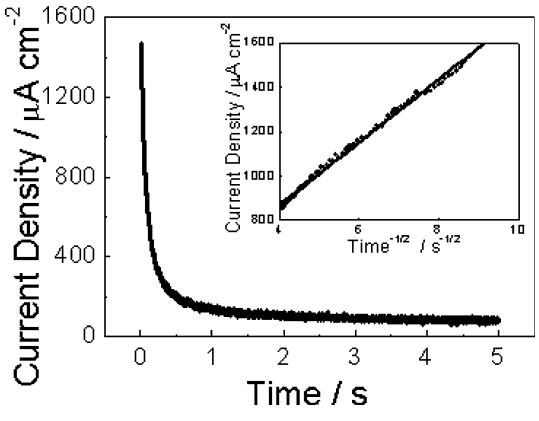

Fig. 7. Transient current density versus time at the potential of −1.0 V in the plating solution composed of 0.5 mM $Pd(NO_3)_2$, 0.033 mM $AgNO_3$, and 2.0 M NH_4NO_3 (pH = 2.6).

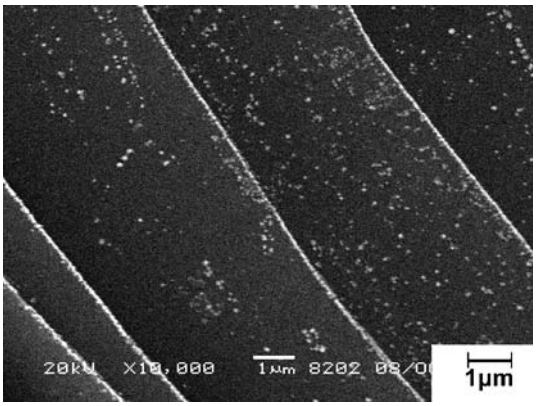

Fig. 8. SEM image of the nanowires obtained on HOPG which was oxidized at 0.8 V for 5 s, followed by nucleation at −1.0 V for 0.6 s.

the grown nanowires became microwires or block if a growth current density was applied beyond $-60\ \mu A\ cm^{-2}$. In this case, discontinuous or dotted wires with a wide diameter distribution were obtained instead of smooth nanowires.

There are different open circuit potentials (OCP) on various samples of HOPG owing to surface state difference. If nanowires grow at a constant potential E_{grow}, the polarization is difficult to establish for each experiment. The different growth overpotentail is probably produced under the same growth potential on different samples. The application of a too positive E_{grow} sometimes reduces the rate of nanowire growth and hinders the coalescence of the nanoparticles into smooth nanowires. In contrast, nanowires with large diameters and discontinuous or nanoparticle features on terraces can be obtained by growth at a high overpotential. The galvanostatic method is found to be useful for producing uniform and continuous nanowires.

The experimental data have shown that the plating solution and the electrodeposition conditions can allow us to synthesize alloy nanowire arrays with the composition of 75–80% Pd and 20–25% Ag. The average nanowire diameter ranges from 109 nm (Figure 10A) to 430 nm (Figure 10B and C). The SEM images of Pd–Ag nanowire arrays in Figures 9 and 10 demonstrate that the nanowire arrays are continuous, parallel, ordered, and well-aligned.

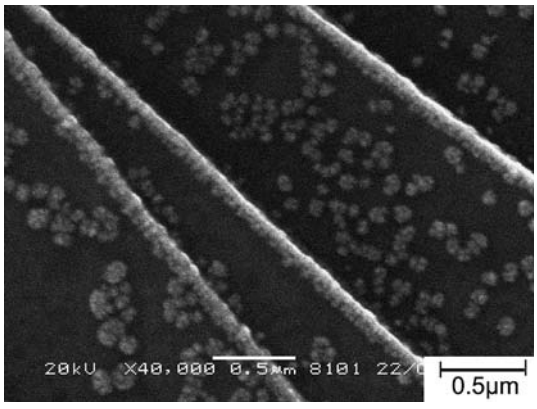

Fig. 9. SEM image of nanowires obtained by growing for 600 s at a current density of $-20\ \mu A\ cm^{-2}$ ($E_{ox} = 1$ V, $t_{ox} = 20$ s, $E_{nucl.} = -1.0$ V, $t_{nucl.} = 0.6$ s, $c_{Pd} = 0.5$ mM, $c_{Ag} = 0.033$ mM, pH = 2–3).

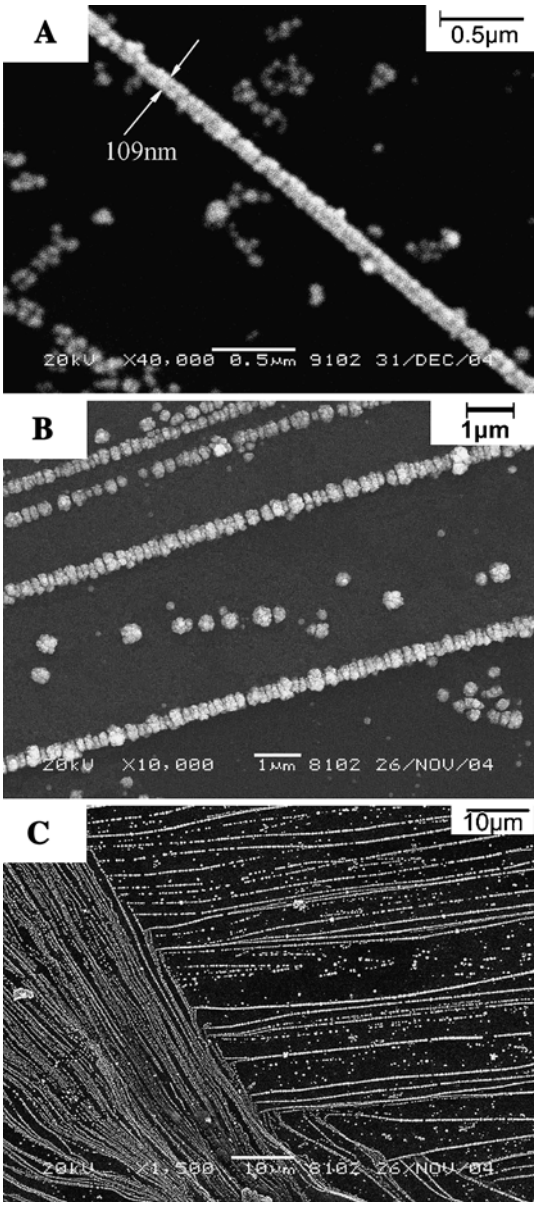

Fig. 10. Typical SEM images showing the morphologies of the Pd–Ag alloy nanowire arrays (A: $-20\ \mu A\ cm^{-2}$ for 600 s; B and C: $-60\ \mu A\ cm^{-2}$ for 1200 s).

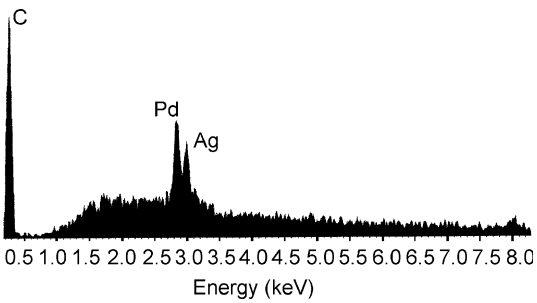

Fig. 11. Energy-dispersed X-ray spectrum for the alloy nanowires shown in Figure 10B.

Table 2. Electrolyte and electrodeposition conditions for the preparation of Pd–Ag alloy nanowire arrays

Plating solution	Electrodeposition Parameter values		
$Pd(NO_3)_2$ 0.5 mM $AgNO_3$ 0.033 mM NH_4NO_3 2 M pH 2–3	E_{ox}/time 1.0 V_{SCE}/ 20 s	E_{form}/time −1.5 V_{SCE} /0.6 s	i_{grow}/time −20 μA cm^{-2}/ 600 s (in Figure 10A) −60 μA cm^{-2}/ 1200 s (in Figure 10B, C)

The composition spectrum of alloy nanowire arrays in Figure 10B obtained by Energy dispersed X-ray spectrometer (EDX) analysis is shown in Figure 11. It shows that the mass ratio of Pd and Ag in the alloy is 77:23.

4. Conclusion

In conclusion, some new insights have been gained for the preparation of Pd–Ag alloy nanowires, which are useful for further development of hydrogen sensors. The main conclusions are summarized as follows:

1. Pd–Ag alloy nanowires can be electrodeposited on HOPG from a plating solution composed of $Pd(NO_3)_2$, $AgNO_3$, and NH_4NO_3 by the control of oxidation potential (0.8–1.1 V_{SCE}), the nucleation potential (−1.0 to −1.5 V_{SCE}) and the growth current (−20 to −60 μA cm^{-2}). The morphologies of the alloy nanowire arrays are continuous, parallel, ordered, and well-aligned.
2. The composition of alloy nanowires is controlled by adjusting the concentration ratio of palladium and silver. The composition of 75–80% Pd and 20–25% Ag in the alloy nanowires has been obtained in the 0.5 mM $Pd(NO_3)_2$ plating solution with a Pd/Ag concentration of 15:1.
3. The concentration of 2 M NH_4NO_3 in the plating solution has been found to be a optimal concentration, which play important roles in increasing the solution conductance and in providing complexing agent for the co-deposition of palladium and silver ions.

Acknowledgements

Financial supports of this research by the National Science Foundation of China (Grant No. 20373015) and Hunan Education Office (Grant No. 04C033) are appreciated.

References

1. K.Scharnagl,M.Eriksson,A.Karthigeyan,M.Burgmair,M.Zimmer and I. Eisele, *Sens. Actuators B.* **78** (2001) 138.
2. M. Yun, N.V. Myung, R.P. Vasquez and J. Wang, *Nanofabrication Technol. in* Dobisz and A. Elizabeth (Eds), Proceedings of the SPIE, 5220 (2003) 37.
3. E.C. Walter, F. Favier and R.M. Penner, *Anal. Chem.* **74** (2002) 1546.
4. F. Favier, E.C. Watler, M.P. Zach, T. Benter and R.M. Penner, *Science* **293** (2001) 2227.
5. G. Kaltenpoth, P. Schnabel, E. Menke, E.C. Walter, M. Grunze and R.M. Penner, *Anal. Chem.* **75** (2003) 4756.
6. J.V. Zoval, J. Lee, S. Gorer and R.M. Penner, *J. Phys. Chem. B.* **102** (1998) 1166.
7. J. Li, Y. Lu, Q. Ye, M. Cinke, J. Han and M. Meyyappan, *Nano Lett.* **3** (2003) 929.
8. Y. Wang, G. Meng, L. Zhang, C. Liang and J. Zhang, *Chem. Mater.* **14** (2002) 1773.
9. M.P. Zach, K.H. Ng and R.M. Penner, *Science* **290** (2000) 2120.
10. S.Z. Chu, K. Wada, S. Inoue and S. Todoroki, *Chem. Mater.* **14** (2002) 4595.
11. Y.W. Wang, L.D. Zhang, G.W. Meng, X.S. Peng, Y.X. Jin and J. Zhang, *J. Phys. Chem. B.* **106** (2002) 2502.
12. Y. Guo, L. Wan, C.F. Zhu and D.L. Yang, *Chem. Mater.* **15** (2003) 664.
13. C. Ji and P.C. Searson, *J. Phys. Chem. B.* **107** (2003) 4494.
14. I. Mukhopadhyay and W. Freyland, *Langmuir* **19** (2003) 1951.
15. M.D. Lay and J.L. Stickney, *J. Am. Chem. Soc.* **125** (2003) 1352.
16. S. Hou, C. Tao and Z. Xue, *Chin. Sci. (Vol. E).* **31** (2001) 213.
17. D. Djalali, S.Y. Li and M. Schmidt, *Macromolecules* **35** (2002) 4282.
18. Y. Xiong, Z. Li, R. Zhang, Y. Xie, J. Yang and C. Wu, *J. Phys. Chem. B.* **107** (2003) 3697.
19. W.R. Han and J. Zhu, *Chin. J. Nonferrous Metals* **8** (1998) 406.
20. Y. Fukumoto, Y. Kawashima, K. Handa and Y. Hayashi, *Metal Finishing* **9** (1984) 77.
21. E.C. Walter, B.J. Murray, F. Favier, G. Kaltenpoth, M. Grunze and R.M. Penner, *J. Phys. Chem. B.* **106** (2002) 11407.
22. R.J. Rice and R.L. McCreery, *Anal. Chem.* **61** (1989) 1637.
23. R.J. Bowling, R.L. McCreery, C.M. Pharr and R.C. Engstrom, *Anal. Chem.* **61** (1989) 2763.
24. R.S. Robinson, K. Sternitzke, M.T. McDermott and R.L. McCreery, *J. Electrochem. Soc.* **138** (1991) 2412.
25. B.R. Scharifker, *J. Electroanal Chem.* **458** (1998) 253.